



PAPER • OPEN ACCESS

A binary motor imagery tasks based brain-computer interface for two-dimensional movement control

To cite this article: Bin Xia *et al* 2017 *J. Neural Eng.* **14** 066009

View the [article online](#) for updates and enhancements.

Related content

- [A combination strategy based brain-computer interface for two-dimensional movement control](#)
Bin Xia, Oladazimi Maysam, Sandra Vesper *et al.*
- [The hybrid BCI system for movement control by combining motor imagery and moving onset visual evoked potential](#)
Teng Ma, Hui Li, Lili Deng *et al.*
- [Enhancing performance of a motor imagery based brain-computer interface by incorporating electrical stimulation-induced SSSEP](#)
Weibo Yi, Shuang Qiu, Kun Wang *et al.*

A binary motor imagery tasks based brain-computer interface for two-dimensional movement control

Bin Xia^{1,2}, Lei Cao^{1,3}, Oladazimi Maysam⁵, Jie Li³, Hong Xie¹, Caixia Su⁴
and Niels Birbaumer²

¹ Shanghai Maritime University, 201306 Shanghai, People's Republic of China

² Institute of Medical Psychology and Behavioral Neurobiology, University of Tuebingen, D-72074 Tuebingen, Germany

³ Tongji University, 201804 Shanghai, People's Republic of China

⁴ Shengze Hospital of Jiangsu Province, 215228 Jiangsu, People's Republic of China

⁵ Werner Reichardt, Center for Integrative Neuroscience (System Neurophysiology), University of Tuebingen, D-72076 Tuebingen, Germany

E-mail: binxia@shmtu.edu.cn

Received 2 November 2016, revised 6 July 2017

Accepted for publication 11 July 2017

Published 10 November 2017



Abstract

Objective. Two-dimensional movement control is a popular issue in brain-computer interface (BCI) research and has many applications in the real world. In this paper, we introduce a combined control strategy to a binary class-based BCI system that allows the user to move a cursor in a two-dimensional (2D) plane. Users focus on a single moving vector to control 2D movement instead of controlling vertical and horizontal movement separately. **Approach.** Five participants took part in a fixed-target experiment and random-target experiment to verify the effectiveness of the combination control strategy under the fixed and random routine conditions. Both experiments were performed in a virtual 2D dimensional environment and visual feedback was provided on the screen. **Main results.** The five participants achieved an average hit rate of 98.9% and 99.4% for the fixed-target experiment and the random-target experiment, respectively. **Significance.** The results demonstrate that participants could move the cursor in the 2D plane effectively. The proposed control strategy is based only on a basic two-motor imagery BCI, which enables more people to use it in real-life applications.

Keywords: brain-computer interface, motor imagery, 2-dimensional movement control

(Some figures may appear in colour only in the online journal)

1. Introduction

In the past decades, the brain-computer interface (BCI) has received considerable attention because it is a novel communication tool or control channel between the brain and the external world that does not use the peripheral nervous system or muscles [1–8]. BCIs are especially useful for patients with

motor impairments (e.g. motor neuron degenerative diseases and paralysis) [9–13].

Cursor control is a popular model in BCI research. The ability to control cursor movements using brain responses allows for different applications, such as surfing the internet and spelling [14–16] to be run conveniently and make it a very desirable tool. Additionally, cursor control can be easily implemented and quantified. Cursor control can also serve as a prototype for testing a new paradigm or algorithm [17]. In previous studies, research focused on one-dimensional cursor control, which allows the participant to control either vertical or horizontal movement [18–21]. Recently, two-dimensional



Original content from this work may be used under the terms of the [Creative Commons Attribution 3.0 licence](https://creativecommons.org/licenses/by/3.0/). Any further distribution of this work must maintain attribution to the author(s) and the title of the work, journal citation and DOI.

(2D) cursor control has been introduced which enables the user to control a considerably enhanced interface [22–24]. Generally, invasive BCIs achieve more precise movement control because of the higher signal-to-noise ratio of the brain signal acquired from action potentials or local field potentials; however, there are some substantial technical difficulties and significant clinical risks [25, 26]. By contrast, electroencephalography (EEG)-based non-invasive BCI is safer and more comfortable to apply, and could be performed by every individual with no special competence [27–29]. Wolpaw *et al* [30] used a non-invasive based BCI to train four participants to control a 2D cursor control with a motor imagery (MI) paradigm, and the participants achieved good performance. This pioneering study inspired more researchers to develop 2D cursor control systems using EEG-based BCI [31, 32], such as steady-state visual evoked potential (SSVEP), P300, event related desynchronization/synchronization (ERD/S) [30, 33, 34].

Recently, hybrid strategies have been used in 2D movement control to exploit different combined BCI approaches. Li *et al* [35] combined an motor imagery (MI) and visual attention approach to extract the ERD and P300 to control horizontal movement and vertical movement, respectively. In another study [36], the authors combined ERD and SSVEP to control 2D movement.

In previous studies, single modality and multi-modality BCIs demonstrated good performance in 2D control experiments; however, most of these BCIs applied complex control strategies with a heavy workload [17]. We developed a three-class MI-based BCI for 2D control; however, some participants failed to control a three-class MI simultaneously in these experiments [24]. Developing an easy-to-use 2D control strategy based on a single EEG modality is still a challenging issue. In this work, we use two-class MI tasks to develop a 2D movement control system. A novel combination strategy is introduced, which allows the participant to control 2D movement by controlling the combination of two-class MI tasks in a rotating coordinate system (RCS). Experimental results and further data analysis demonstrate the high performance compared with other state-of-the-art BCI-based 2D movement control systems.

2. Materials and methods

2.1. Participants

Ten healthy adults (all right-handed; four females and six males, age range 20–26 years, average age 23 years) were recruited to participate in the experiment. All participants were free of neurological or psychiatric disorders. Participant 1 and participant 2 had prior experience in MI-based BCIs, and the other participants had no prior experience. Prior to the experiment and after they received overall information about the nature of the experiment, all participants signed an informed consent form. They received 15 RMB per hour for their participation.

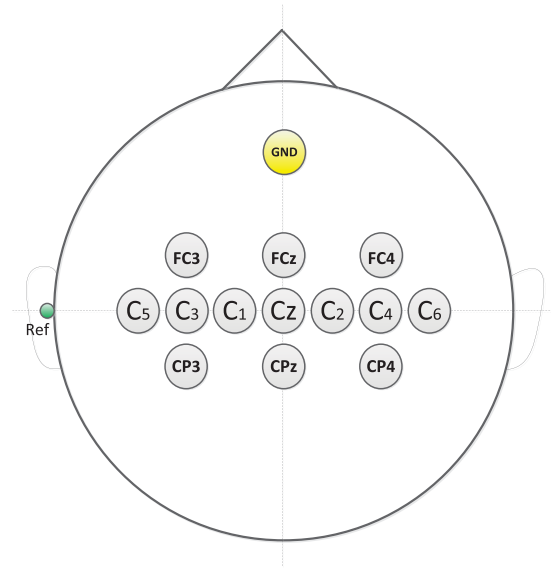


Figure 1. Electrode distribution used for EEG data acquisition.

2.2. Data acquisition

EEG data were acquired using a Gtec Amplifier (g.tec, Graz, Austria), with a sample rate of 256 Hz and with a band-pass filter of 5–30 Hz. To fully cover the motor cortex area for all participants, 13 electrodes at the standard positions of the 10–20 international system [37] (FC3 FCz FC4 C5 C3 C1 Cz C2 C4 C6 CP3 CPz CP4) (figure 1) were used for signal acquisition. The number of electrodes can be reduced for specific participants in further studies. The ground was fixed on the AFz and a reference electrode was located at the left earlobe.

2.3. Control paradigm

In a normal two-class MI-based BCI system, the participant is required to perform one task at a time. The BCI system calculates two posterior probabilities, which represent the two MI tasks, and provides a predict label (e.g. 1 or –1) according to the higher probability. In this work, we used a left hand and right hand MI-based BCI system. **Posterior probabilities (p_1 , p_2) were applied to construct a 2D movement control system instead of discrete labels.** For the first step, the posterior probabilities were projected into two vectors (P_1 , P_2) in a 2D plane. As shown in figure 2(b), the P_1 was projected from probability p_1 , and the norm was equal to p_1 . P_2 was projected from p_2 in the same manner. P_1 and P_2 were placed on the left-hand side and right-hand side of the Y_0^R axis at a fixed 60° angle. In the experiment, the projected vectors that numerically translated from probabilities P were produced trial by trial. In the i th trial, P_1^i and P_2^i were the projected vectors that represented the probabilities related to the left and right hand imagery, respectively.

As shown in figure 2(b), the initial velocity vector V_0 was combined by vector P_1^0 and P_2^0 , which moved the cursor from position S_0 to S_1 in a step (trial) time (step time = 100 ms). After the first step, if P_1 and P_2 were projected in the same

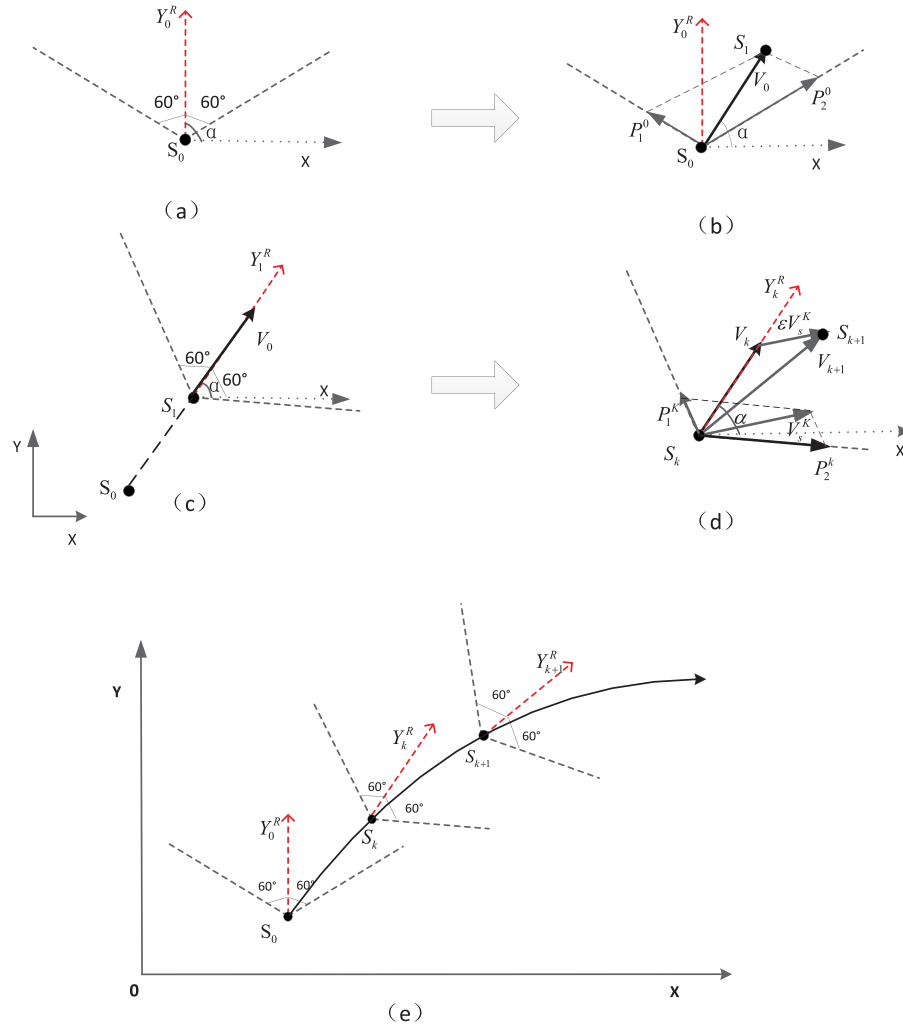


Figure 2. Illustration of the combination strategy. (a) Initial position of the RCS, which is in coincident with the absolute coordinate system. Y_0^R represents the vertical axis and X represents the horizontal axis. Two dotted lines indicate the projected directions and S_0 is the starting point of the cursor. α is the angle between the Y_k^R axis of the RCS and the positive horizontal axis of the absolute coordinate system. (b) First velocity vector V_0 is combined with P_1^0 and P_2^0 . (c) RCS moved from S_0 to S_1 and Y_1^R in the direction of V_0 . (d) Demonstration of how to generate V_{k+1} from V_k (current velocity vector) and V_s^K (The combination of probabilities). (f) The RCS moving with the cursor's trajectory.

direction as the initial position, the velocity vector could only move the cursor in the area between P_1 and P_2 . To move the cursor toward any position in the 2D plane, we used an RCS that moved along the current velocity vector. As shown in figure 2(c), the origin of the RCS moved from S_0 to S_1 and Y_1^R in the direction of V_0 . Figure 2(e) shows that RCS moved along the trajectory of the cursor. Figure 2(d) demonstrates how to generate the velocity vector V_{k+1} , which moved the cursor from S_k to S_{k+1} . The current velocity is V_k , and V_s^K is the new vector generated by probabilities. Then the next velocity vector V_{k+1} is a combination of V_k and V_s^K defined as following:

$$V_{k+1} = \varepsilon V_s^K + V_k \quad (1)$$

where $\varepsilon (< 1)$ is an attenuation parameter, which is an empirical parameter to limit the speed of the cursor. In this paper, we chose $\varepsilon = 0.1$ for all participants.

To calculate the coordinates of the cursor in an absolute coordinates system, we need to determine the relationship

between the RCS and absolute coordinate system. For the first step, the origin is coincident with both coordinates. The coordinates of the cursor are calculated as

$$X_0 = V_{0x}b \quad (2)$$

$$Y_0 = V_{0y}b, \quad (3)$$

where b is the step length. To limit the speed of the cursor, step length b is set to 8 pixels. For the second step, the coordinates are calculated as

$$\begin{aligned} X_k &= X_{k-1} + V_{kx}b \\ &= X_{k-1} + [\varepsilon P_2^k \cos(\pi/3 - \alpha) \\ &\quad + \varepsilon P_1^k \cos(\pi/3 + \alpha)]b \end{aligned} \quad (4)$$

$$\begin{aligned} Y_k &= Y_{k-1} + V_{ky}b \\ &= Y_{k-1} + [\varepsilon P_2^k \sin(\pi/3 - \alpha) \\ &\quad + \varepsilon P_1^k \sin(\pi/3 + \alpha)]b \end{aligned} \quad (5)$$

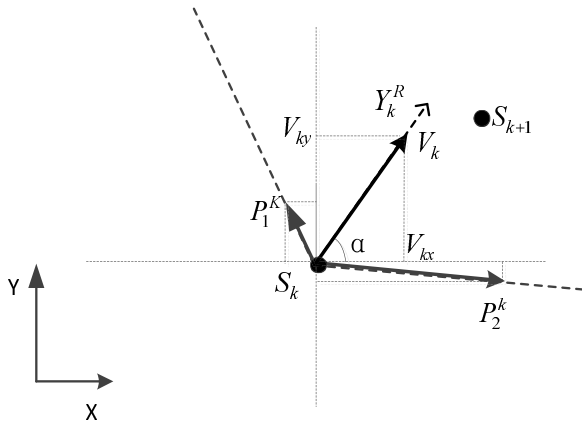


Figure 3. Illustration the relationship between RCS and absolute coordinate system.

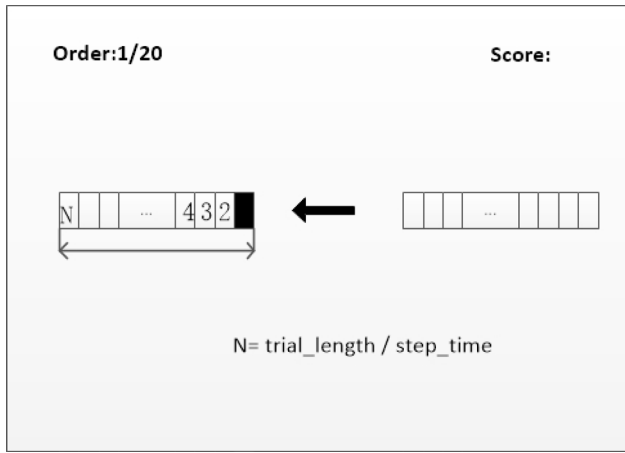
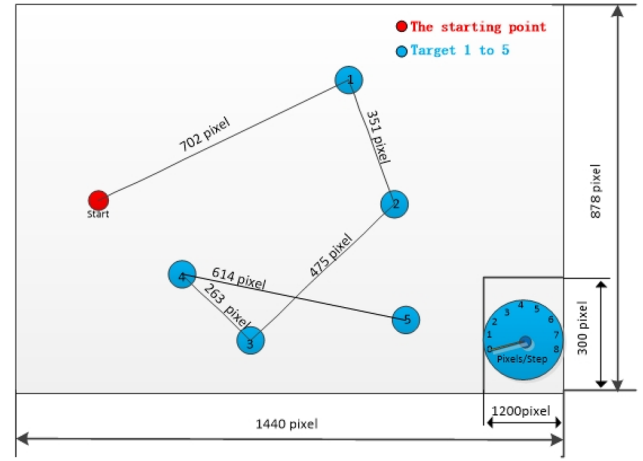


Figure 4. Illustration the bar filling paradigm for two motor imagery tasks. Left bar and right bar represent the left and right hand MI, respectively. Both bars were divided into N subbars using the trial time divided by the step time. When the participant performed one MI task, one subbar was filled depending on the classification result.

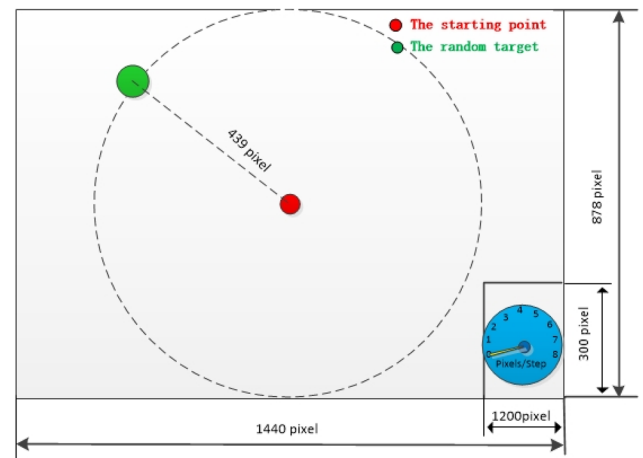
where X_{k-1} and Y_{k-1} are the previous coordinates; V_{kx} and V_{ky} are the projection of V_k on the horizontal and vertical axes, respectively; and α is the angle between the Y_k^R axis of the RCS and the horizontal positive axis of the absolute coordinate system (figure 3), where α is calculated as follows

$$\alpha = \arctan \frac{S_{(k-1)y} - S_{(k-2)y}}{S_{(k-1)x} - S_{(k-2)x}}. \quad (6)$$

The control procedure is similar to our previous work [24], in which participants were instructed to control a combination of probabilities by performing one MI task or two MI tasks simultaneously; however, the main difference is the number of combinations. In [24], participants switched between three types of combination (left hand and right hand, left hand and foot, right hand and foot) according to specific target. However, participants only need to control one combination (left hand and right hand) in the proposed system, which greatly reduces the difficulty of the control task.



(a)



(b)

Figure 5. Illustration of the experimental environment. (a) Five-fixed target experiment, (b) Five-random target experiment.

Table 1. Experimental results of the five-fixed targets experiment.

Participant	Trials	Hit rate (%)	Ratio
1	75	100	1.11
2	75	100	1.40
3	75	100	1.25
5	75	100	1.32
9	50	92	3.24
Mean		98.9	1.48

To build the proposed paradigm based 2D control BCI system, the common spatial pattern (CSP) [38] was applied to extract the features of two MI tasks and a linear support vector machine (SVM) classifier was trained to discriminate the different MI patterns. However, the outputs of standard SVM are discrete labels. In order to obtain the posterior probabilities, Platt proposed a method for a standard SVM [40], and this method was implemented in the LIBSVM toolbox [39]. In the LIBSVM toolbox, to output the posterior probabilities, we needed to set the $-b$ parameter in the training and testing function. We applied a grid search method to determine the best parameters, and used five-fold cross-validation.

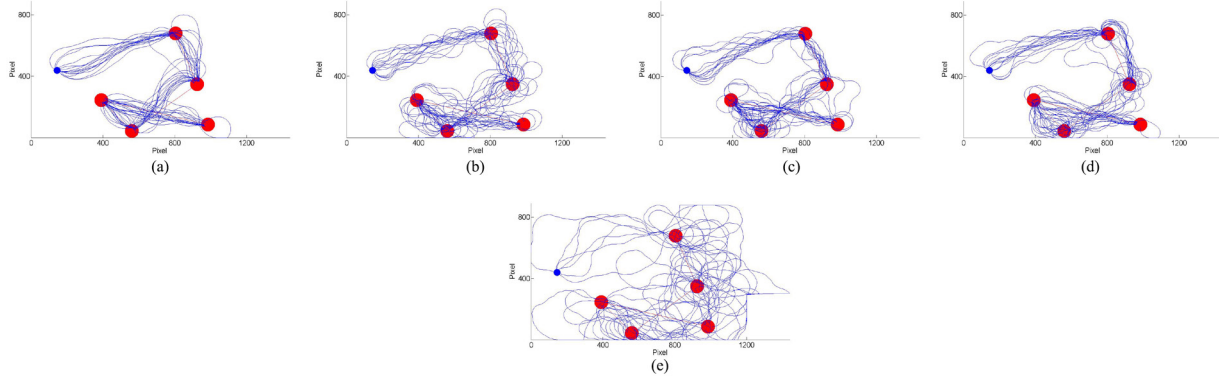


Figure 6. The cursor trajectories in the five-fixed target experiment for five subjects. (a) Participant 1. (b) Participant 2. (c) Participant 3. (d) Participant 5. (e) Participant 9.

Table 2. The average time for each target in the five-fixed targets experiment. The bold type indicates that the shortest time for each target among five subjects.

Parti	Target 1 (s)	Target 2 (s)	Target 3 (s)	Target 4 (s)	Target 5 (s)
1	11.9 ± 0.5	6.9 ± 1.4	9.3 ± 1.5	4.8 ± 1.4	11.3 ± 5.6
2	12.9 ± 1.5	10.0 ± 5.0	13.7 ± 6.0	5.3 ± 1.2	13.1 ± 2.6
3	12.9 ± 0.9	6.9 ± 2.7	14.1 ± 7.8	5.5 ± 2.5	11.9 ± 4.1
5	13.0 ± 3.2	10.0 ± 4.3	12.4 ± 4.5	5.3 ± 0.7	11.1 ± 1.8
9	32.4 ± 18.3	31.7 ± 17.1	32.5 ± 14.2	10.3 ± 6.0	20.9 ± 14.3

2.4. Experimental procedure

The experiment consisted of two conditions: the five-fixed target experiment and the five-random target experiment. Before the two experiments, the participants took part in an MI training session. In the training and 2D control experiments, all participants were instructed to imagine moving their left (right) hand to fill the left (right) side bar or move the cursor to the left (right).

2.4.1. Motor imagery training.

All participants were required to take part in two-class MI training (left versus right hand movement imagery). As shown in figure 4, the participants performed MI to fill the bar (divided N subbar, where N is the step number) following the direction of the arrow. Each trial lasted 3 s, divided into 30 steps, with a step time of 0.1 s. The selection criterion was that the performance for left and right hand imagery for three consecutive runs (each run included 20 trials) was over 85%. If the participants could not achieve the selection criterion within five training sessions, they were not allowed to participate in the subsequent experiment.

2.4.2. Online 2D experimental conditions. The participants had to perform two experimental tasks. In both conditions the experimental screen size was a rectangle of 1440×878 pixels figure 5(a). In the lower right area of 240×300 pixels, a speedometer with a maximum speed of 8 pixels was depicted. A red dot indicated the cursor and blue dots represented the targets. The workspace was $1440 \times 878 - 240 \times 300$ pixels. The ratio of the size of the cursor to the size of the target and workspace was 0.00048:0.0022:1.

In the five-fixed target experiment, we placed five targets in a fixed sequence figure 5(a). For each run, the objective was for the participant to hit all five targets from target 1 to target 5. At the beginning of each task, a 3 s countdown clock timer was shown at the center of the screen to indicate the start of the tasks, meanwhile the color of the current target changed to green. If the participant controlled the cursor to hit a target within 60 s, the next trial would start immediately with another 3 s countdown timer. Otherwise, the system would terminate the trial after 60 s and start the next trial. All participants were required to repeat the experiment 15 times.

The aim of the five-random target experiment was to verify that the participant could move the cursor to any position without a fixed routine. In this experiment, the initial position of the cursor was at the center of the screen. After a 3 s countdown, a green target appeared in a random position with a distance of 439 pixel from the current cursor position figure 5(b). If the participant could not complete a trial within 60 s, the system stopped the current trial and the next trial started. The next target appeared at any position within a range of 439 pixels from the current cursor position. All participants were required to repeat the experiment 15 times.

3. Results

All participants attended the training session, but only five participants (1, 2, 3, 5 and 9) met our selection criterion, that is, an average accuracy of three consecutive runs over 85%.

Four participants finished two experiments (15 runs for each condition) and one participant attended 10 runs only in both condition experiments due to a personal reason. Table 1 shows the experimental results of the five-fixed targets experiment including the hit rate and the trajectory ratio (the mean trajectory versus the shortest trajectory). Four participants achieved 100% hit rate with a small trajectory ratio. Participant 1 achieved the best trajectory ratio which is coincide with the trajectories shown in figure 6. Even the trajectory ratio of participant 9 was the biggest compared with the other participants, he also achieved a high hit rate. In table 2, the average time for each target is depicted. Participant 1 outperformed other participants in target 1, 3, 4. In addition, the performances of participant 1 in the other two remaining

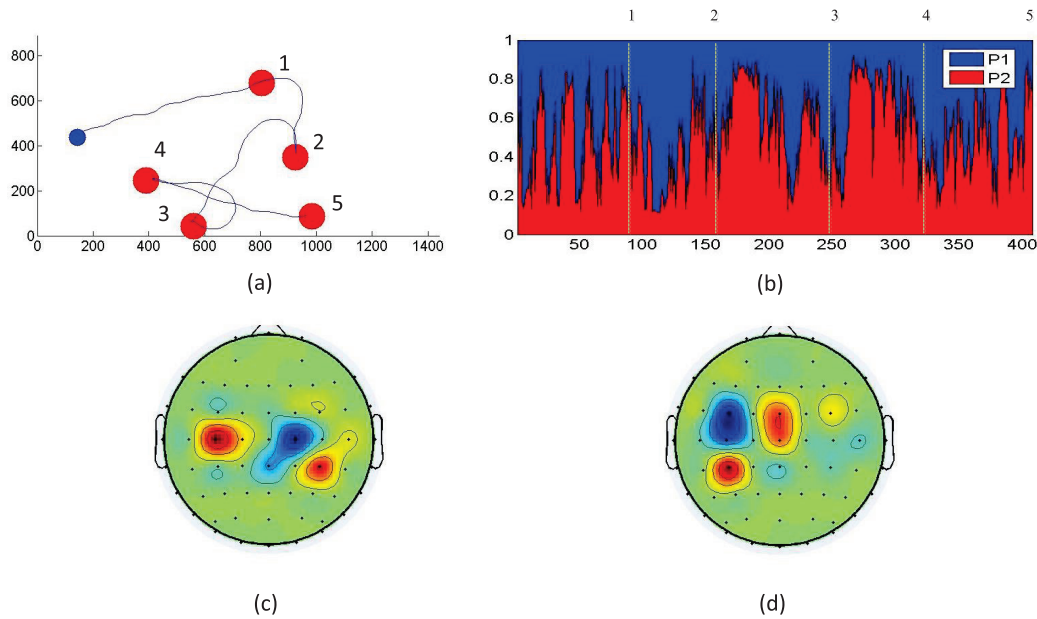


Figure 7. Demonstration of the five-fixed targets experiment (Participant 5). (a) The trajectory from one experiment. (b) The combination of probabilities when the participant moved the cursor to hit the target from 1 to 5, where p_1 (p_2) represented left (right) hand MI-related posterior probability (c) Scalp maps of the selected CSP filter for left hand. (c) The scalp map of selected CSP filter for right hand.

Table 3. Results of the five-random targets experiment.

Participant	Trials	Hit rate (%)	Average task time (s)	Ratio
1	75	100	8.9 ± 1.7	1.23
2	75	100	10.0 ± 3.5	1.38
3	75	100	10.1 ± 4.2	1.39
5	75	100	8.8 ± 2.0	1.20
9	50	96	19.3 ± 12.5	2.96
Mean		99.4	11.1 ± 7.3	1.48

targets were comparable to the best performer of the respective target. Figure 7 demonstrated that the participant was able to apply a different combination of two MI tasks to move the cursor to a specific target.

The specificity of the five-random targets experiment was that the participant could not prepare for the next target until he or she had finished the current target. Table 3 summarises the results of the five-random targets experiment including the hit rate, the average time and trajectory ratio. The performance of all participants was satisfactory.

4. Discussion

In this study, we present a combination strategy based 2D cursor control system which allows participant to perform the 2D cursor control by combining two different MI tasks (right hand motor imagery and left hand motor imagery). In order to demonstrate the utility of the proposed system, we set the selection criterion for the training session quite high (85%), to ensure that our paradigm could be tested without the risk that low MI performance was caused by little training practice. Five participants successfully completed the training session and participated in the five-fixed targets and five-random targets experiments. As shown above, all

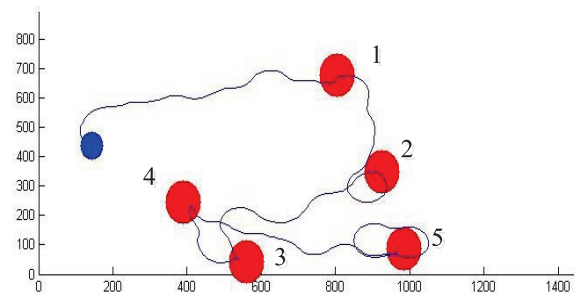


Figure 8. Illustration of short distance problem.

participants achieved high performance in both experiments. At the beginning of each trail, the initial velocity vector always points upward fixed with the initial mapping position. Afterwards, the participant needs to adjust the cursor to the direction of the target by concentrating on one MI task. When the cursor point to the target direction, the participant moves the cursor in a straight fashion to reach the target by controlling the combination of two MI tasks. As shown in figure 5(a), participant 1 controls the tasks very well and moves the cursor with a short trajectory ratio (The trajectory ratio of Participant 1 is 1.11. The more the ratio is close to 1, the more trajectory is close to a straight line). In this work, we hypothesized that participants are able to employ one MI task or simultaneous two MI tasks to control the combination of probabilities. Figure 7(b) shows how the participant controls different combinations of probabilities to move the cursor to hit different targets. Comparing the hit rates and trajectory ratios in both experiments, the participants achieved similar results. Even participant 9, whose performance in the five-fixed target experiment was the worst, performed better in the five-random target experiment. After the experiments, the participants told us that the unpredictability of the target inspired their motivation.

Wolpaw proposed three criterions to measure the performance on a point-to-point movement: movement time (i.e. the lower the better); movement precision (i.e. the target size as a percentage of workspace; the smaller the better); hit rate (percent of targets reached in the time allotted; the higher the better) [30]. Although the number of targets and the control strategy differs in our work, we all share the goal of controlling 2D point-to-point movement and was comparable in terms of success in achieving this goal. In [30], the best hit rate was 78% for healthy participants, which is less than the lowest hit rate in our work, and Wolpaw *et al*'s movement precision was 4.9% greater than 0.22% achieved in our present study (the movement precision the smaller the better), so their movement times were shorter (1.9s compared to the average times shown in table IV and V). In our previously study [24], a three-class MI based control strategy was employed to control 2D movement. The participants achieved high performance but they also experienced heavy workload to perform the three-class MI task. In the current work, the performance is similar but the workload is reduced because the participants need to control the combination of two MI tasks only. Compared with the hybrid BCI, Li *et al* [35] realized 2D cursor control by combining MI and P300 and achieved success rates of 84.5%–97.5%, which is a range that is substantially lower than the hit rate accuracy in the proposed five-fixed target experiment. Furthermore, our movement precision is smaller than their 0.3%. In another hybrid work [36] employed the MI to control the vertical position and SSVEP to control the horizontal position, the average accuracy over all participants was around 60%. These hybrid studies realized 2D control, but time was consumed to detect or trigger P300 and SSVEP compared with motor imagery. Moreover P300 and SSVEP cause visual fatigue. For single modality-based BCI, such as the SSVEP or P300, the same drawbacks occur, and the discrete commands also cause the cursor to move in a zigzag routine.

For long distance targets in both experiments (the shortest distance between two targets is 263 pixels.), five participants achieved high performance. However, with the proposed system it is difficult to move the cursor to hit a target located at a short distance. As shown in figure 2(d), the cursor only changes direction within a limited range. Therefore, the cursor does not hit the target if it is located within a short distance e.g. 20 pixels and is also outside the direction range that the cursor can reach. Figure 8 shows the cursor approaching the target 2 that is located at a short distance from the cursor and is also out of the cursors direction range, the participant can only move the cursor to turn a long curve to hit the target. However, this limitation is beneficial for some application, like wheel chair control. Using the proposed control strategy, user can control wheel chair to change the direction smoothly and avoid changing direction sharply.

5. Conclusion

We proposed a 2D control system with a combination strategy of two-class MI tasks. Participants were instructed to focus on controlling combinations of probabilities while performing

one or two MI tasks simultaneously. In two types of online control experiments, the preselected participants ranked high in their performance.

Acknowledgments

The work was supported by the National Natural Science Foundation of China (Grant Nos. 31450110072, 61550110252) and the Shanghai Committee of Science and Technology, China (Grant No. 14441900300), Shanghai Maritime University Foundation, Deutsche Forschungsgemeinschaft (DFG, Kosellek), Stiftung Volkswagenwerk (VW), Brain Products, Gilching and German Center of Diabetes Research (DZD) at University of Tuebingen, Eva and Horst Koehler Stiftung, Baden-Wrternberg-Stiftung.

References

- [1] Wolpaw J R, Birbaumer N, McFarland D J, Pfurtscheller G and Vaughan T M 2002 Brain-computer interfaces for communication and control *Clin. Neurophysiol.* **113** 767–91
- [2] Birbaumer N, Ghanayim N, Hinterberger T, Iversen I, Kotchoubey B, Kübler A, Perelmouter J, Taub E and Flor H 1999 A spelling device for the paralysed *Nature* **398** 297–8
- [3] De Massari D, Ruf C A, Furdea A, Matuz T, Van Der Heiden L, Halder S, Silvoni S and Birbaumer N 2013 Brain communication in the locked-in state *Brain* **136** 1989–2000
- [4] Li J, Liang J, Zhao Q, Li J, Hong K and Zhang L 2013 Design of assistive wheelchair system directly steered by human thoughts *Int. J. Neural Syst.* **23** 1350013
- [5] Li J, Ji H, Cao L, Zang D, Gu R, Xia B and Wu Q 2014 Evaluation and application of a hybrid brain computer interface for real wheelchair parallel control with multi-degree of freedom *Int. J. Neural Syst.* **24** 1450014
- [6] Zhang Y, Zhou G, Jin J, Zhao Q, Wang X and Cichocki A 2014 Aggregation of sparse linear discriminant analyses for event-related potential classification in brain-computer interface *Int. J. Neural Syst.* **24** 1450003
- [7] Vidal J-J 1973 Toward direct brain-computer communication *Ann. Rev. Biophys. Bioeng.* **2** 157–80
- [8] Vidal J J 1977 Real-time detection of brain events in EEG *Proc. IEEE* **65** 633–41
- [9] Bozinovski S, Sestakov M and Bozinovska L 1988 Using EEG alpha rhythm to control a mobile robot *Proc. of the Annual Int. Conf. of the IEEE Engineering in Medicine and Biology Society* (<https://doi.org/10.1109/IEMBS.1988.95357>)
- [10] Bozinovski S 1990 Mobile robot trajectory control: from fixed rails to direct bioelectric control *Proc. of the IEEE Int. Workshop on Intelligent Motion Control* vol 2 (IEEE) pp 463–7
- [11] Mueller-Putz G R, Pokorny C, Klobassa D S and Horki P 2013 A single-switch brain-computer interface based on passive and imagined movements: towards restoring communication in minimally conscious patients *Int. J. Neural Syst.* **23** 1250037
- [12] Ortiz-Rosario A and Adeli H 2013 Brain-computer interface technologies: from signal to action *Rev. Neurosci.* **24** 537–52
- [13] Ortiz-Rosario A, Berrios-Torres I, Adeli H and Buford J A 2014 Combined corticospinal and reticulospinal effects on upper limb muscles *Neurosci. lett.* **561** 30–4
- [14] Yu T, Li Y, Long J and Gu Z 2012 Surfing the internet with a BCI mouse *J. Neural Eng.* **9** 036012

- [15] Xia B, Yang J, Cheng C and Xie H 2013 A motor imagery based brain-computer interface speller *Advances in Computational Intelligence* (Berlin: Springer) pp 413–21
- [16] Nakanishi M, Wang Y, Wang Y-T, Mitsukura Y and Jung T-P 2014 A high-speed brain speller using steady-state visual evoked potentials *Int. J. Neural Syst.* **24** 1450019
- [17] Faller J, Müller-Putz G, Schmalstieg D and Pfurtscheller G 2010 An application framework for controlling an avatar in a desktop-based virtual environment via a software SSVEP brain-computer interface *Presence: Teleoperators Virtual Environments* **19** 25–34
- [18] McFarland D J, Sarnacki W A and Wolpaw J R 2003 Brain-computer interface (BCI) operation: optimizing information transfer rates *Biol. Psychol.* **63** 237–51
- [19] Cheng M, Jia W, Gao X, Gao S and Yang F 2004 Mu rhythm-based cursor control: an offline analysis *Clin. Neurophysiol.* **115** 745–51
- [20] Fabiani G E, McFarland D J, Wolpaw J R and Pfurtscheller G 2004 Conversion of EEG activity into cursor movement by a brain-computer interface (BCI) *IEEE Trans. Neural Syst. Rehabil. Eng.* **12** 331–8
- [21] McFarland D J and Wolpaw J R 2005 Sensorimotor rhythm-based brain-computer interface (BCI): feature selection by regression improves performance *IEEE Trans. Neural Syst. Rehabil. Eng.* **13** 372–9
- [22] Li Y, Wang C, Zhang H and Guan C 2008 An EEG-based BCI system for 2D cursor control *IEEE Int. Joint Conf. on Neural Networks* (IEEE World Congress on Computational Intelligence) pp 2214–9
- [23] Long J, Li Y, Yu T and Gu Z 2012 Target selection with hybrid feature for BCI-based 2D cursor control *IEEE Trans. Biomed. Eng.* **59** 132–40
- [24] Xia B, Maysam O, Veser S, Cao L, Li J, Jia J, Xie H and Birbaumer N 2015 A combination strategy based brain-computer interface for two-dimensional movement control *J. Neural Eng.* **12** 046021
- [25] Hochberg L R, Serruya M D, Friehs G M, Mukand J A, Saleh M, Caplan A H, Branner A, Chen D, Penn R D and Donoghue J P 2006 Neuronal ensemble control of prosthetic devices by a human with tetraplegia *Nature* **442** 164–71
- [26] Jin J, Allison B Z, Zhang Y, Wang X and Cichocki A 2014 An ERP-based BCI using an oddball paradigm with different faces and reduced errors in critical functions *Int. J. Neural Syst.* **24** 1450027
- [27] Taylor D M, Tillery S I H and Schwartz A B 2002 Direct cortical control of 3D neuroprosthetic devices *Science* **296** 1829–32
- [28] Wolpaw J R, Loeb G E, Allison B Z, Donchin E, do Nascimento O F, Heetderks W J, Nijboer F, Shain W G and Turner J N 2006 BCI meeting 2005-workshop on signals and recording methods *IEEE Trans. Neural Syst. Rehabil. Eng.* **14** 138–41
- [29] Zhang Y U, Zhou G, Jin J, Wang X and Cichocki A 2014 Frequency recognition in SSVEP-based BCI using multisets canonical correlation analysis *Int. J. Neural Syst.* **24** 1450013
- [30] Wolpaw J R and McFarland D J 2004 Control of a two-dimensional movement signal by a noninvasive brain-computer interface in humans *Proc. Natl Acad. Sci. USA* **101** 17849–54
- [31] McFarland D J, Todd Lefkowitz A and Wolpaw J R 1997 Design and operation of an EEG-based brain-computer interface with digital signal processing technology *Behav. Res. Methods Instrum. Comput.* **29** 337–45
- [32] McFarland D J, Krusienski D J, Sarnacki W A and Wolpaw J R 2008 Emulation of computer mouse control with a noninvasive brain-computer interface *J. Neural Eng.* **5** 101
- [33] Piccione F, Giorgi F, Tonin P, Priftis K, Giove S, Silvoni S, Palmas G and Beverina F 2006 P300-based brain computer interface: reliability and performance in healthy and paralysed participants *Clin. Neurophysiol.* **117** 531–7
- [34] Trejo L J, Rosipal R and Matthews B 2006 Brain-computer interfaces for 1D and 2D cursor control: designs using volitional control of the EEG spectrum or steady-state visual evoked potentials *IEEE Trans. Neural Syst. Rehabil. Eng.* **14** 225–9
- [35] Li Y, Long J, Yu T, Yu Z, Wang C, Zhang H and Guan C 2010 A hybrid BCI system for 2D asynchronous cursor control *Annual Int. Conf. of the IEEE Engineering in Medicine and Biology Society* (IEEE) pp 4205–8
- [36] Allison B Z, Brunner C, Altstätter C, Wagner I C, Grissmann S and Neuper C 2012 A hybrid ERD/SSVEP BCI for continuous simultaneous two dimensional cursor control *J. Neurosci. Methods* **209** 299–307
- [37] Niedermeyer E and Lopes da Silva F H 2005 *Electroencephalography: Basic Principles, Clinical Applications and Related Fields* (Philadelphia: Lippincott Williams and Wilkins)
- [38] Ramoser H, Müller-Gerking J and Pfurtscheller G 2000 Optimal spatial filtering of single trial EEG during imagined hand movement *IEEE Trans. Rehabil. Eng.* **8** 441–6
- [39] Chang C-C and Lin C-J 2011 LIBSVM: a library for support vector machines *ACM Trans. Intell. Syst. Technol.* **2** 27
- [40] Platt J et al 1999 Probabilistic outputs for support vector machines and comparisons to regularized likelihood method *Adv. Large Margin Classif* **10** 61–74